Measuring Photon Time Spread Distribution of Scintillators on the Picosecond Time Scale

J. T. M. de Haas, E. v.d. Kolk, and P. Dorenbos

***Abstract*—In the search for scintillators that have a faster response than existing ones, better knowledge on the processes that take place during the first 100 ps of the scintillation process is required. For that one needs detailed information on the intrinsic rise time of a scintillation pulse. However, the observed rise time, also of direct importance to the timing resolution, is strongly affected by the time spread of photons leaving the scintillator. In this work we pioneered the use of a 120 fs Ti-sapphire laser in combination with a streak camera system to measure those photon time spreads with time resolution up to 5 ps. With this setup the photon time spread distributions of scintillator crystals with different size and/or surface treatment were measured. The potential to study the effect of Teflon packaging on this distribution was also investigated.**

***Index Terms*—Scintillation detectors, time resolution, time-of-flight PET.**

I. Introduction

FOR TOF-PET scanners scintillation detectors are desired that have a better timing performance than existing ones. An important property that determines the timing performance is the intrinsic rise time of the scintillation pulse [1]–[4]. Depending on the point of origin and internal reflections at the crystal interfaces, different photons travel different optical paths before they leave the crystal. There will be a spread in photon exit times. In this work this spread is referred to as the photon time spread distribution. Because of such time spread the observed rise time will be less steep than the intrinsic one. In order to determine and study the intrinsic rise time, the photon time spread distribution needs to be known.

An experimental setup has been built that consists of a 120 fs Ti-sapphire laser system in combination with a streak camera system. The laser pulse produces a light pulse in the scintillator of which the photon time spread distribution is registered by the streak camera with about 5 ps time resolution. In this work the setup is presented, and first results on the photon time spread distribution in $Lu_2SiO_5 : Ce^{3+}$ (LSO:Ce) and $(Lu, Y)_2SiO_5 : Ce$ (LYSO:Ce) scintillation pixels are presented. The set-up is not yet optimized for scintillator studies. Our aim in this work is to demonstrate that this new tool can provide valuable information on the effect of crystal shape and size, its surface condition, and the reflector on the photon time spread distribution.

Manuscript received May 24, 2013; revised September 05, 2013; accepted October 28, 2013. Date of publication January 09, 2014; date of current version February 06, 2014.

The authors are with the Faculty of Applied Sciences, Department Radiation Science and Technology, Section FAME-LMR Delft University of Technology, 2629 JB Delft, The Netherlands (e-mail: J.T.M.deHaas@TUDelft.nl).

Color versions of one or more of the figures in this paper are available online at http://ieeexplore.ieee.org.

Digital Object Identifier 10.1109/TNS.2013.2288693

II. Experimental Methods

To measure the photon time spread distribution, the fs laser pulses were aimed on a spot on one of the surfaces of the scintillating pixel. The wavelength of the laser was tuned around 420 nm, i.e. the same as the main emission wavelength of the used LYSO:Ce and LSO:Ce scintillators. The photons enter the crystal on one side and will leave without or, due to scattering, after several internal reflections on the side facing the streak camera and will be detected by this camera. A mode-locked Ti:sapphire laser system, providing femtosecond pulses of about 120 fs full width half maximum (FWHM), is used. It consists of a Coherent, Inc., model Mira 900F mode locked laser, pumped by a 10 W Coherent, Inc., Verdi V-10 laser. In combination with a frequency doubler or tripler system, one may generate pulses with a wavelength between 270 to 900 nm. A Hamamatsu 5680 streak camera was used in the so-called synchroscan mode. There are 4 time ranges in this mode with a sweep duration of 120 ps, 800 ps, 1.5 ns and 2.2 ns and with a time resolution of 5, 20, 40 and 60 ps, respectively. A more detailed description of the laser system and streak camera can be found in [5]. Fig. 1 illustrates the configuration of the scintillator in front of the streak camera. Because the laser beam diverges slightly, a diaphragm of 0.3 mm was placed about 3 cm before the scintillator face. A narrow tube of $\emptyset 1 \times 6$ mm^2 between the front surface of the sample and the streak camera projects part of the photons from the front face onto the entrance slit of the streak camera. In future studies we intent to use a well-aligned pinhole geometry or a lens system for proper imaging. Then also accurate (x,y,z) positioning tools for the sample and for accurate alignments of the laser beam, the sample, imaging system and streak camera input optics will be implemented.

Four scintillation crystals that differ in size and/or surface treatment were studied. For a depolished (a diffuse surface, usually produced by chemical etching, sandblasting, etc.) $3 \times 3 \times 5$ mm^3 LYSO:Ce crystal the time spread distribution was measured as a function of the spot hit by the laser along a 5 mm long face of an unpacked crystal. The same experiment was done for an all side polished $3 \times 3 \times 5$ mm^3 LSO:Ce crystal wrapped in Teflon tape reflective layers as a function of the number of layers. The distribution was also measured for different size and surface treatments of the crystal. For the Teflon wrapped scintillators the laser light needs to travel through the Teflon layers before entering the crystal. In this work the time spread caused by those Teflon layers was also studied.

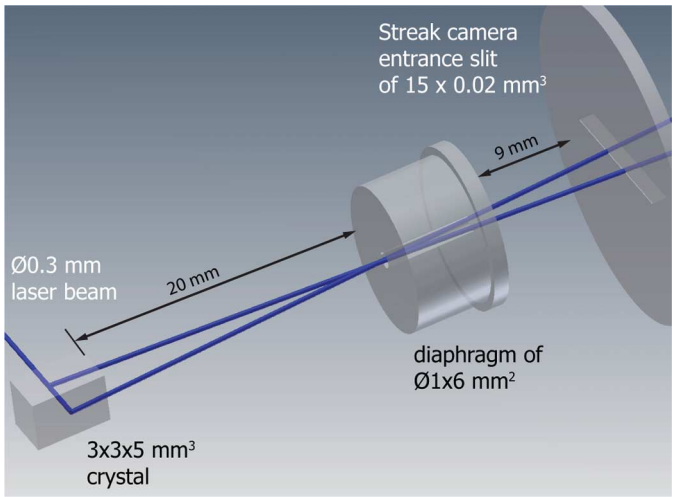

Fig. 1. Illustration of the laser-scintillator-camera configuration.

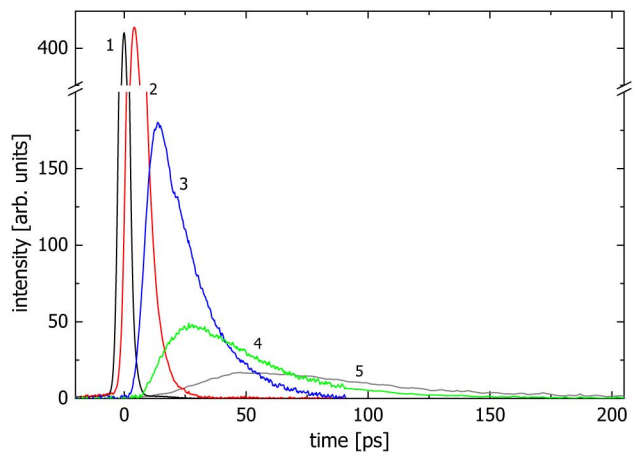

Fig. 2. Broadening and delay of the laser pulse as function of the number of Teflon layers. Curve 1 shows the laser pulse, line 2 to 5 are for 1 to 4 layers of 0.1 mm thick Teflon tape, respectively.

III. Results and Discussion

A. Time Spread in Teflon Tape

ERIKS Eriflon standard 12×0.1 mm^2 Teflon tape was used to measure the time spread of the laser pulse when traveling through this tape as a function of the number of layers. The measurement was done in transmission, i.e. the laser pulse hits one side of the tape and on the other side the difference in traveling time of the photons through the tape is measured by the streak camera. For 1 and 2 layers, range 1 of the synchroscan mode was used. For 3 layers the first 100 ps was recorded in range 1 and the longer times in range 2. The time spread through four layers of Teflon tape was only measured in range 2. The results are shown in Fig. 2. With increasing of the number of layers the FWHM of the distribution increases from 8 ps to 80 ps. The maximum shifts from 4 ps to 47 ps. Clearly the photons are delayed inside the Teflon layers due to multiple photon scattering leading to broadening of the distribution.

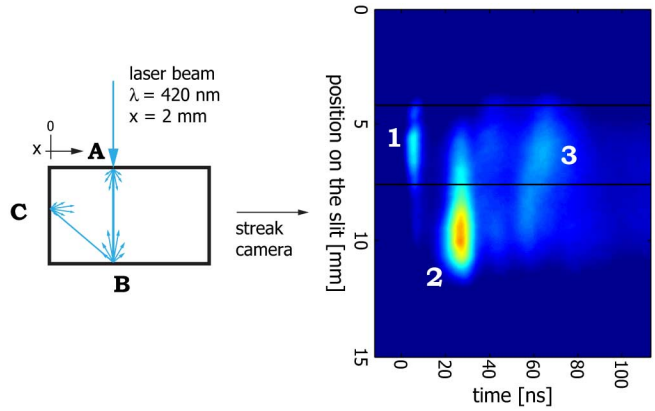

Fig. 3. Streak image of a $3 \times 3 \times 5$ mm^3 unpacked depolished LYSO:Ce pixel at $x = 2$ mm.

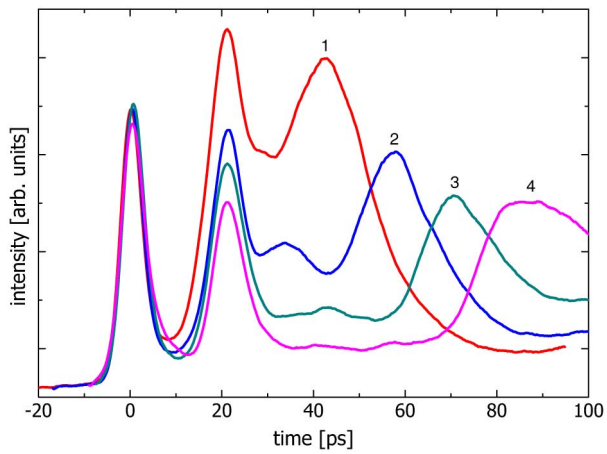

Fig. 4. Photon time spread profiles recorded between slit positions 5 and 7.5 mm for a depolished LYSO:Ce pixel. Profiles recorded for the laser beam incident at points $x = 1$, 2, 3, and 4 mm are shown by curves 1 to 4, respectively.

B. Time Spread From a Depolished LYSO:Ce Pixel

An all side depolished $3 \times 3 \times 5$ mm^3 LYSO:Ce crystal pixel provided by Saint-Gobain was used to measure in time range 1 the photon time spread distribution. The ø0.3 mm laser beam hits the crystal at spot A located in the center (1.5 mm high) of one of the four 3×5 mm^2 faces at a location x from the back face of the pixel as illustrated in Fig. 3. At four positions x, the photon time spread distribution was recorded.

The streak image shows three main spots. Spot 1 is from photons scattered at point A traveling directly through the $\emptyset 1 \times 6$ mm^2 diaphragm onto the slit of the streak camera. This is the fastest route photons can travel and the arrival time is therefore defined as $t = 0$ ps. Spot 2 is from photons that first travel through 3 mm crystal and then scatter at point B towards the entrance slit. Photons scattered at point B towards the back of the crystal and then scattered in the direction of the streak camera, appear as spot 3 in Fig. 3. The smearing from 60 to about 70 ps is due to the different path lengths travelled by the photons from B to different points at the back face of the crystal. Fig. 4 shows the integral of the streak image intensity between slit position 5 and 7.5 mm, as indicated by the two black lines in Fig. 3, for $x = 1$, 2, 3, and 4 mm. In these time profiles spot 1 is by definition at

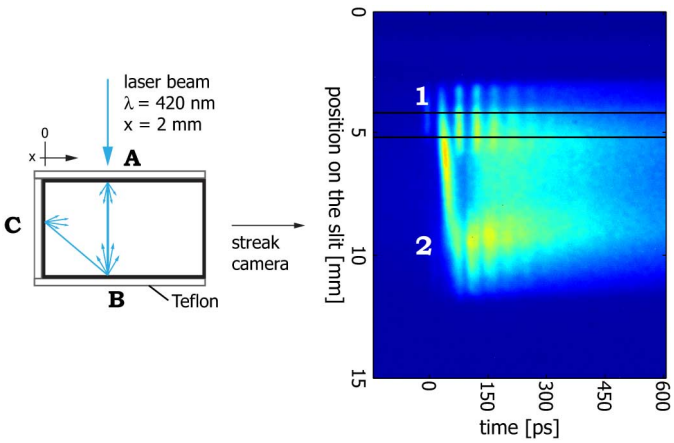

Fig. 5. Streak image of a $3 \times 3 \times 5$ mm^3 polished LSO:Ce pixel covered in five sides with 1 layer of 0.1 mm thick Teflon tape.

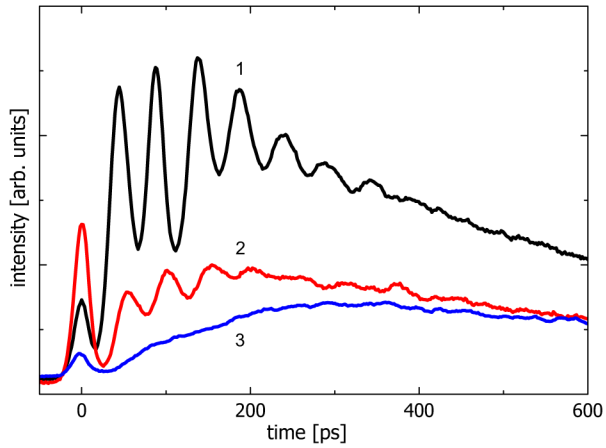

Fig. 6. Photon collection time profiles of a $3 \times 3 \times 5$ mm^3 polished LSO:Ce pixel packed in 1 (curve 1), 2 (curve 2), and 4 (curve 3) layers of Teflon tape.

time zero and spot 2 is, independently of x, 20 ps later, which corresponds to travel time in 3.3 mm path length in LYSO:Ce with a refractive index of 1.82. The difference of 0.3 mm in this path length with the real thickness of the pixel may be due to a small deviation from normal incidence of the laser beam or other misalignments in the set-up. The third main peak shifts from 40 ps for $x = 1$ to about 90 ps for $x = 4$ mm which is directly linked to the increase of path length B-C, see Fig. 3, with increase of x. One even may observe a fourth peak, most prominent at 35 ps for $x = 2$ mm. Most likely these are from photons scattered directly from A via C to the streak camera. Those peaks precede that of photons scattered via B and C again by about 20 ps.

C. Time Spread in a Teflon Wrapped Polished Pixel

An all sides polished $3 \times 3 \times 5$ mm^3 LSO:Ce crystal from Agile was used to study the effect of Teflon packaging on the photon time spread distribution. For these studies time range 2 of the streak camera was used. When Teflon is absent, scattering of photons at the surface is very low and the laser beam will travel straight through the crystal; under such conditions almost no signal is recorded with the streak camera.

Fig. 5 shows the photon streak image from the polished crystal packed on five of its sides in one layer of Teflon tape. The laser is incident at point A at $x = 2$ mm as illustrated in Fig. 5. In essence the image is similar to Fig. 3. However, apparently due to the small amount of scattering at the polished interfaces the photons bounce back and forth between spots A and B. Each time a small fraction is scattered in the Teflon tape towards the streak camera leading to a repetition of peaks at locations 1 and 2 on the entrance slit separated about 22 ps in time.

Curve 1 in Fig. 6 shows the integral of the streak image between slit position 4 and 5 mm as indicated by the two black lines in Fig. 5. One observes the repeated scattering from point A as a series of 8 well resolved peaks each separated 45 ps in time. The same measurements shown as curve 2 and 3 were done for the crystal packed in 2 and 4 layers of Teflon. Note that the time difference between the repeating peaks measured with 2 layers of Teflon tape are about 5 ps longer than that measured with 1 layer. Also the repetition time of the peaks, 45 ps, with one layer of Teflon is somewhat longer than expected from the data of the bare crystal. This provides direct experimental evidence and first data on the time needed for photons to leave the crystal, to scatter inside the Teflon tape, and to re-enter the crystal. Evidently the reflection inside Teflon tape leads to an increase in the photon time spread distribution and is bound to affect the coincidence timing resolution. With 4 layers of Teflon the reflection peaks are totally smeared out in time. This is attributed to the increase of the photon time spread distribution by reflection from and transmission through 4 layers of Teflon, see Fig. 2.

D. The Effect of Pixel Size and Surface Condition

To study the effect of pixel size and surface condition on the photon time spread distribution, four different crystals covered with four layers of Teflon tape on five sides were studied. The same two crystals as in Sections III-B and III-C) plus one $3 \times 3 \times 5$ mm^3 LYSO:Ce pixel from Crystel Photonics where five faces are depolished and one 3×3 mm^2 face was polished. The fourth crystal is a LSO:Ce $3 \times 3 \times 20$ mm^3 from Agile. Both 3×3 mm^2 faces were polished and the 3×20 mm^2 faces were depolished.

Fig. 7 shows the photon time spread distributions of the four studied pixels. Curve (1) for the five sides de-polished and 3×3 mm^2 outgoing (front) face polished LYSO:Ce crystal displays the shortest photon time spread distribution. Curve (2) is for the sample where also the outgoing 3×3 mm^2 face of the crystal is depolished. Apparently a significant larger fraction of the photons are reflected and scattered back into the crystal at the crystal-air interface leading to substantially longer photon collection times on the streak camera. Curve (3) is from the 20 mm long pixel further lengthening the photon time spread distribution. The all sides polished LSO:Ce crystal displays the longest photon time spread distribution. It may take several ns before all photons have left the sample. It is empirically well known that polished pixels display different coincidence timing resolution than depolished ones [6]–[8].

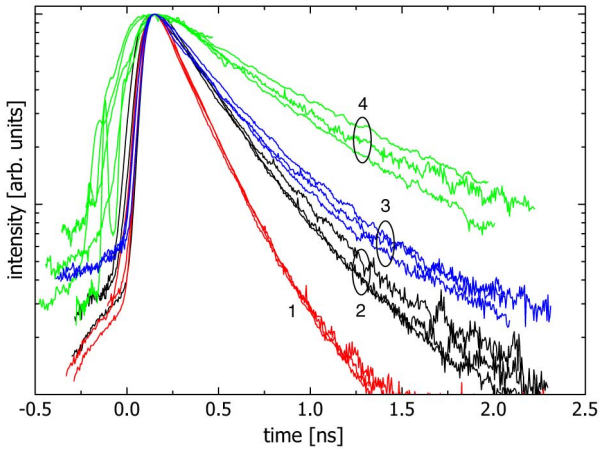

Fig. 7. Photon time spread distributions of the $3 \times 3 \times 5$ mm^3 LYSO:Ce with one 3×3 mm^2 side polished (curve 1), $3 \times 3 \times 5$ mm^3 all sides unpolished LYSO:Ce pixel (curve 2), a $3 \times 3 \times 20$ mm^3 LSO:Ce with both 3×3 mm^2 sides polished (curve 3), and a $3 \times 3 \times 5$ mm^3 all polished LSO:Ce (curve 4).

IV. Summary, Conclusions, and Outlook

The data and figures presented above demonstrate that the combination of a tunable 120 fs pulsed Ti-sapphire laser and a streak camera provides a powerful technique to study the photon time spread distribution of scintillator pixels with about 5 ps time resolution. Part of the photons emerging from the outgoing front face of the pixel were projected by a 1 mm diameter 6 mm long hole onto the entrance slit of the streak camera. This is far from optimal. By constructing a smaller and shallower pinhole or by using a lens system as input optics we aim to obtain a proper imaging of the surface that will provide us better data on the time, position, and angle under which individual photons emerge from the crystal surface.

Photon collection time distributions in scintillators are often simulated by ray tracing software like Geant or Litrani [9]–[11]. They are perfectly able to simulate photon collection times of samples of different geometries, but only under idealized situations. One always needs to enter assumptions on the reflection condition at the crystal reflector interface. One may use Lambert-Beer scattering at almost normal incidence at the interface together with specular reflection at grazing incidence. To what extent this is correct and how one should take into account the time spent inside the reflecting medium and the time spread caused by that is not known. All these aspects are difficult or even impossible to properly take into account without having access to real experimental data. In the case of one or multiple layers of 0.1 mm Teflon we have found, see Fig. 6, that the photons spend significant time inside the Teflon before it re-enters the crystal. It is also unavoidable that the point of re-entry will be different than the point of escape. Such complex reflection aspects are not implemented in ray tracing software, simply because of lack of experimental data to base a simulation upon. The new technique pioneered in this work has the time resolution, and with proper imaging also the position resolution to study those aspects in detail. We furthermore demonstrated that an all sides polished crystal leads to lengthening of the photon collection times as compared to a depolished crystals. This is also known from ray tracing simulation studies but here in this work one observes it in real time, and as such our method can verify or falsify simulated data. Aspects like, what type of reflecting medium at what thickness is optimal for minimal time spread, or to assess the effect and quality of surface treatments on the time spread can also be studied with the new instrumentation.

References

[1] L. G. Hyman, "Time resolution of photomultiplier tube systems," *Rev. Sci. Instr.*, vol. 36, pp. 193–196, Feb. 1965.

[2] S. Seifert, H. T. van Dam, and D. R. Schaart, "The lower bound on the timing resolution of scintillation detectors," *Phys. Med. Biol.*, vol. 57, pp. 1797–814, Mar. 2012.

[3] P. Lecoq, E. Auffray, S. Brunner, H. Hillemanns, P. Jarron, A. Knapitsch, T. Meyer, and F. Powolny, "Factors influencing time resolution of scintillators and ways to improve them," *IEEE Trans. Nucl. Sci.*, vol. 57, no. 5, pp. 2411–2416, Oct. 2010.

[4] W. S. Choong, "The timing resolution of scintillation-detector systems: Monte Carlo analysis," *Phys. Med. Biol.*, vol. 54, pp. 6495–6513, Oct. 2009.

[5] D. J. Louwers, T. Takizawa, C. Hidaka, and E. van der Kolk, "Direct hole and delayed electron capture on a picosecond timescale by Eu^{2+} centers in CaGa2S4 monitored by synchroscan with horizontal blanking," *Appl. Phys*, vol. 111, p. 093709, May 2012.

[6] S. E. Derenzo, M. J. Weber, W. W. Moses, and C. Dujardin, "Measurements of the intrinsic rise times of common inorganic scintillators," *IEEE Trans. Nucl. Sci.*, vol. 47, pp. 860–864, Jun. 2000.

[7] S. Seifert, "Improving the time resolution of TOF-PET detectors by double-sided readout of high-aspect-ratio scintillation crystals," *IEEE Trans. Nucl. Sci.*, to be published.

[8] V. Ch. Spanoudaki and C. S. Levin, "Investigating the temporal resolution limits of scintillation detection from pixellated elements: Comparison between experiment and simulation," *Phys. Med. Biol.*, vol. 56, pp. 735–756, Jan. 2011.

[9] F. X. Gentit, "Litrani: A general purpose Monte-Carlo program simulating light propagation in isotropic or anisotropic media," *Nucl. Instr. Meth. A*, vol. 486, p. 35, 2002.

[10] M. Janecek and W. W. Moses, "Simulating scintillator light collection using measured optical reflectance," *IEEE Trans. Nucl. Sci.*, vol. 57, no. 3, pp. 946–970, Jun. 2010.

[11] E. Roncali and S. R. Cherry, "Simulation of light transport in scintillators based on 3D characterization of crystal surfaces," *Phys. Med. Biol.*, vol. 58, pp. 2185–2198, Mar. 2013.